

Recombination Processes in *p*-Type Indium Antimonide*

R. N. ZITTER, A. J. STRAUSS,† AND A. E. ATTARD‡
Chicago Midway Laboratories, Chicago, Illinois

(Received February 26, 1959)

Photoelectromagnetic and photoconductive lifetimes have been measured from 77° to 300°K in monocrystalline *p*-type indium antimonide of net acceptor concentration ranging from less than 10^{15} cm⁻³ to 10^{18} cm⁻³. It is concluded that at the lower temperatures, excess electrons are trapped in immobile states in the forbidden band and that the trap concentration is the same in all samples, regardless of net acceptor concentration. At intermediate temperatures, trapping becomes negligible but recombination continues to take place through states in the forbidden gap; there is some reason to believe that in this temperature region lifetimes are determined by more than one level of forbidden-band states. At still higher temperatures, where the samples are intrinsic, the lifetime data are consistent with the hypothesis of a direct interband Auger recombination process.

1. INTRODUCTION

IN the course of measurements at this laboratory on single-crystal *p*-type InSb, it became clear that excess carrier lifetimes depend on net acceptor concentrations and not on the particular crystal involved, although some of the crystals were grown years apart, growth rates varied from one crystal to another, and a few crystals were doped with zinc or cadmium while the remainder were not purposely doped. It seemed that a systematic study of how lifetime depends upon net acceptor concentration and temperature might possibly permit identification of the factors, present in all crystals, which govern the recombination processes observed in InSb; also, the measured lifetimes would serve as a base or reference to which the effects on lifetime of heat treatment, doping with impurities, etc., could be compared.

The steady-state photoelectromagnetic (PEM) and photoconductive (PC) effects were used to study recombination for the following reasons: the effects are well suited for measurements of the rather small lifetimes occurring in *p*-type InSb, the PEM effect itself indicates whether or not surface recombination is negligible, and a comparison of the lifetimes obtained from the PEM and PC effects separately shows the extent of excess carrier trapping in immobile states in the forbidden gap.

The lifetimes reported here are believed to be characteristic of the bulk, since surface recombination was not noticeable and the photoresponses after each of several etchings of any one sample were identical. In contrast, reproducibility of the photosignals from *n*-type material at low temperatures after repeated etchings was poor, presumably due to surface effects which could not be controlled. As a consequence, this paper reports only lifetimes in *p*-type material.

* This research was supported by the U. S. Air Force through the Office of Scientific Research of the Air Research and Development Command.

† Present address: Lincoln Laboratory, Lexington, Massachusetts.

‡ Present address: Department of Physics, Illinois Institute of Technology, Chicago, Illinois.

2. MATERIALS AND APPARATUS

Single crystals pulled from the melt supplied all of the samples, which were bridge-shaped, 1.3 cm long, 0.13 cm wide, and between 10^{-2} and 10^{-1} cm thick. Indium was used as solder, and a water-diluted mixture of approximately five parts hydrogen peroxide ("Superoxol") to one part hydrofluoric acid was used as an etch.

For experiments at 77°K, samples were immersed directly in liquid nitrogen in a Pyrex Dewar equipped with Pyrex windows; for 300°K experiments, the samples were placed in a brass container whose wall temperature was maintained by water pumped from a constant-temperature bath. Intermediate temperatures were obtained with Pyrex-windowed Dewars constructed after a published design.¹

Tungsten lamps served as sources of illumination. Essentially monochromatic 1- μ light for 77°K experiments resulted from a combination filter consisting of GaAs and 5 cm of water; it was simple then to compute the photon flux density incident on the samples from the measured response of a tiny calibrated barium titanate thermal detector placed at the position normally occupied by a sample. Correction factors were applied to account for partial reflection at sample surfaces and also, in the case of 77°K measurements, for the difference between the refractive indices of air and liquid nitrogen, since the thermal detector was operated in air at room temperature while the samples were to be immersed in liquid nitrogen.

The light through the 1- μ filter was not sufficiently intense for 300°K photoresponse measurements, so a Nernst glower without filters was used and the photon flux was computed under the assumption that the glower approximates a black-body source.

Illumination was chopped at 1600 cps and the resulting photosignals were transferred by an impedance-matching transformer to a preamplifier and wave analyzer. Each sample was bridge-shaped, and the ends were masked so that illumination fell only on that section of the sample between the so-called potential arms of the bridge. After each measurement or set of

¹ R. W. Ure, Rev. Sci. Instr. 28, 836 (1957).

measurements, the illumination was cut off and a 1600-cps signal of known current was applied to the arms; in other words, a current generator was substituted in place of illumination. In this way, absolute photocurrents could be deduced directly from wave analyzer readings without explicit consideration of the amplification factor involved. This procedure was particularly useful in those PEM measurements where considerable magnetoresistance occurred, since the over-all gain of the system depends on sample resistance and so would be different for each magnetic field.

3. EXPERIMENTAL PROCEDURES AND RESULTS

In the calculation of lifetimes from steady-state PC or PEM effect data, values for the carrier mobilities are required; they were measured according to procedures described in the following text.

(a) Mobilities at 77°K

At 77°K all of the samples are extrinsic *p*-type. Net acceptor concentrations were computed as $(eR_H)^{-1}$ and hole mobilities as the product of Hall coefficient (at 5000 gauss) and zero-field conductivity.

Mobilities of the minority electrons were obtained from PEM data. According to Kurnick and Zitter,² the PEM current per unit sample width in extrinsic *p*-type material at the magnetic field B is given in mks units by

$$i_{PEM} = eI\mu BL_D / (1 + \mu^2 B^2)^{1/2}, \quad (1)$$

where e is the electronic charge, I the photon flux density, μ the electron mobility, and L_D the electron diffusion length. A data-plot of $(B/i_{PEM})^2$ vs B^2 gives a straight line, and μ is just the square root of the ratio

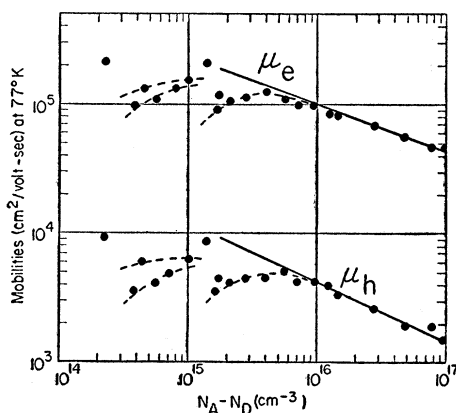


FIG. 1. Mobilities in *p*-type InSb at 77°K. The dashed curves, each of which connects the data of samples from a single grown crystal, show the effect of donor-acceptor compensation on mobility. Presumably, the solid lines represent mobilities in uncompensated material. In all samples the ratio of electron to hole mobility is 25 ± 3 .

² S. W. Kurnick and R. N. Zitter, *J. Appl. Phys.* **27**, 278 (1956).

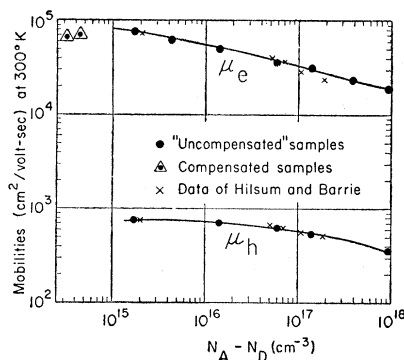


FIG. 2. Mobilities at 300°K. The compensated samples have total impurity concentrations near 2×10^{15} cm^{-3} .

of the line's slope to intercept. (InSb, unlike Ge and Si, has $\mu B \gtrsim 1$ at moderate magnetic fields.) The plot will not be a straight line if surface recombination is important.

Figure 1 shows the results of 77°K mobility measurements over a wide range of net acceptor concentrations. Each of the dotted curves in the figure connects the data of samples taken from a single grown crystal. An obvious interpretation of these curves is that they show the effect on mobility of donor-acceptor compensation. The mobilities in uncompensated material probably are close to the solid lines drawn in the figure.

It may be noted that the electron mobilities in *p*-type InSb consistently are lower by 30% to 40% than mobilities in *n*-type material at corresponding impurity concentrations.³ Qualitatively, this can be attributed to electron-hole scattering.

An outstanding fact to be drawn from the data of Fig. 1 is that at 77°K the ratio of electron to hole mobility b is essentially constant in all the samples; its value is

$$b = 25 \pm 3, \quad (2)$$

regardless of net acceptor concentration or total impurity concentration. This fact will be useful later on in the analysis of lifetime data.

(b) Mobilities at 300°K

Figure 2 shows the mobilities of various samples at 300°K. The degree of donor-acceptor compensation can be inferred from the samples' mobilities at 77°K. As indicated in the figure, only two of the samples are appreciably compensated; each of these probably has a total impurity concentration about 2×10^{15} cm^{-3} .

Mobility measurements at 300°K in InSb are complicated because of mixed conduction. Kurnick and Zitter's² general expressions for PEM response, Hall

³ A. J. Strauss, *J. Appl. Phys.* **30**, 559 (1959).

coefficient, and magnetoresistance are

$$i_{PEM} = \frac{eI\mu BL_D(1+c)^{\frac{1}{2}}(1+1/b)}{[1+\mu^2 B^2 + bc(1+\mu^2 B^2/b^2)]^{\frac{3}{2}}}, \quad (3)$$

$$R_H = \frac{1}{ep_0} \frac{1-b^2c}{(1+bc)^2} \left[1 + \mu^2 B^2 \left(\frac{1-c}{1-b^2c} \right) \right] / \left[1 + \mu^2 B^2 \left(\frac{1-c}{1+bc} \right)^2 \right], \quad (4)$$

$$\frac{\rho_B}{\rho_0} = \left[1 + \mu^2 B^2 \left(\frac{1+c/b}{1+bc} \right) \right] / \left[1 + \mu^2 B^2 \left(\frac{1-c}{1+bc} \right)^2 \right], \quad (5)$$

where $c = n_0/p_0$ is the ratio of equilibrium carrier concentrations. In the same notation, the zero-field conductivity may be written as

$$\sigma_0 = e\mu p_0(1+bc)/b. \quad (6)$$

The above equations simplify considerably for the cases of *p*-type extrinsic material ($c \cong 0$), and nearly intrinsic material ($c \cong 1$). In the extrinsic case, the procedure for measuring mobilities is identical to that used for 77°K data: The product $R_H\sigma_0$ is just the hole mobility, while PEM data give the electron mobility. On the other hand, for intrinsic material the situation is almost reversed in that $R_H\sigma_0$ gives the electron mobility and PEM (or magnetoresistance) data provide a quantity from which the hole mobility is readily computed.

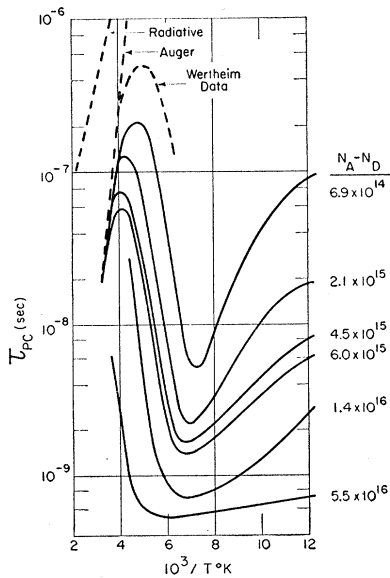


FIG. 3. PC lifetime vs reciprocal temperature for various net acceptor concentrations. Wertheim's results for a sample with $N_A - N_D = 3.0 \times 10^{14} \text{ cm}^{-3}$ are included. At high temperatures, the lifetime deduced by Landsberg and Beattie for direct interband Auger recombination agrees with the data, while the lifetime calculated for direct radiative recombination does not.

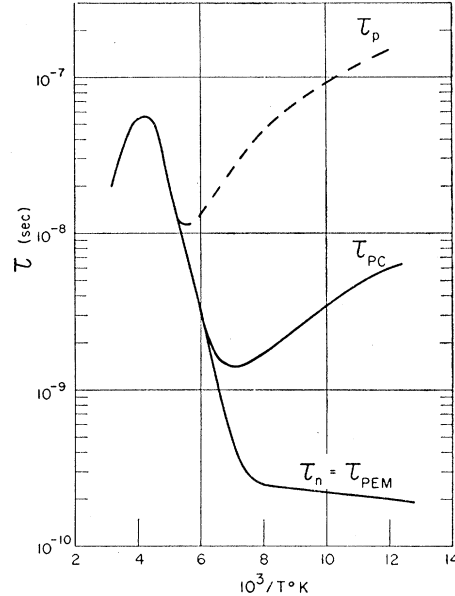


FIG. 4. Lifetime vs reciprocal temperature for a single sample with $3 \times 10^{15} \text{ cm}^{-3}$ net acceptors. The electron and hole lifetimes, τ_n and τ_p , are inferred from the measured quantities τ_{PEM} and τ_{PC} .

The intrinsic concentration of carriers in InSb at 300°K is $2 \times 10^{16} \text{ cm}^{-3}$. At this temperature, a sample with 10^{15} cm^{-3} net acceptors is very nearly intrinsic while a sample with 10^{18} cm^{-3} net acceptors is extrinsic. Therefore all the end points of the mobility curves shown in Fig. 2 are determined by comparatively simple procedures.

The intermediate points are another matter. The approach used in the present work was to expand (4) and (5) as series in B^2 or $1/B^2$. The data for very small and very large magnetic fields could then be plotted against the sum of the first two terms in each series in the manner described earlier in connection with Eq. (1), and the mobilities are computed from slopes and intercepts.

Hilsum and Barrie⁴ made Hall and magnetoresistance measurements on *p*-type InSb at 300°K and, with the use of Eqs. (4), (5), and (6) and extensive curve-fitting, analyzed the data in an elegant manner. Their results are indicated in Fig. 2, and the agreement between the two sets of data is satisfying.

Incidentally, Hilsum and Barrie also showed that Kurnick and Zitter's theoretical model, which is not inconsistent with the assumption of a constant relaxation time independent of energy, fits the 300°K Hall and magnetoresistance data better than the usual models of transport phenomena where the relaxation time varies as some power of the energy. Kurnick and Zitter formed a similar conclusion from the PEM data of *p*-type InSb at 77°K. There is at present no suitable

⁴ C. Hilsum and R. Barrie, Proc. Phys. Soc. (London) **71**, 676 (1958).

explanation for the success of the simple model mentioned above.

(c) Mobilities at Intermediate Temperatures

Once mobilities at 77° and 300°K are determined, it is possible to estimate values at intermediate temperatures from the mobility *vs* temperature data of Howarth *et al.*⁵ and Hrostowski *et al.*⁶ Since the mobilities do not change by more than a factor of two over the entire temperature range, the error in estimating mobilities in this manner is much smaller than the experimental error involved in photocurrent measurements; in short, the estimated values are sufficiently accurate for the calculation of lifetimes.

(d) Carrier Lifetimes

From (3) it is clear that when PEM data are plotted in the form $(B/i_{PEM})^2$ *vs* B^2 , the result is a straight line. The PEM lifetime can be calculated from either the slope or the intercept of the line when the mobilities are known.

The PC lifetime is obtained from the expression²

$$i_{PC} = (1 + 1/b)eI\mu E\tau_{PC}, \quad (7)$$

where i_{PC} is the photoconductive short-circuit current per unit sample width, E is the component of the applied electric field along the sample's length, and the rest of the symbols have the meanings given earlier.

It is well known that if trapping of excess carriers occurs, the PEM and PC lifetimes do not necessarily coincide. It has been shown⁷ in general that the lifetimes

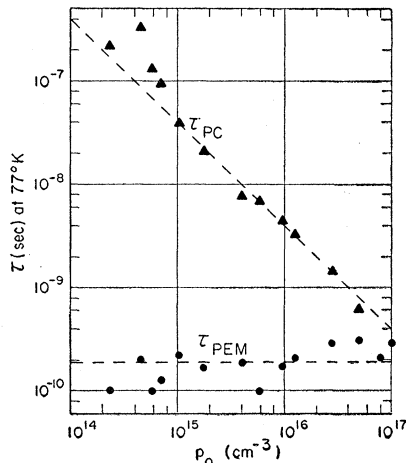


FIG. 5. PEM and PC lifetime *vs* hole concentration at 77°K. τ_{PC} varies as $1/\rho_0$, while τ_{PEM} is independent of ρ_0 .

⁵ Howarth, Jones, and Putley, Proc. Phys. Soc. (London) **B70**, 124 (1957).

⁶ Hrostowski, Morin, Geballe, and Wheatley, Phys. Rev. **100**, 1672 (1955).

⁷ R. N. Zitter, Phys. Rev. **112**, 852 (1958).

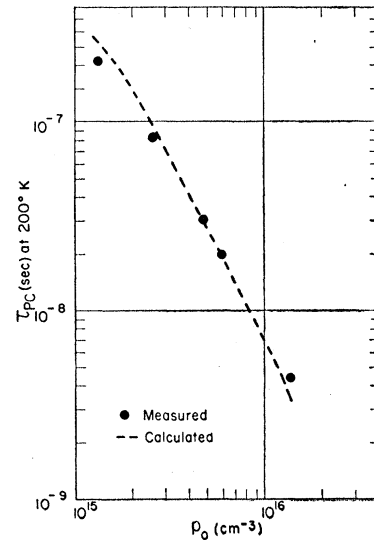


FIG. 6. PC lifetime *vs* hole concentration at 200°K. The dashed curve is calculated from (19), with $\tau_{p0} = 8 \times 10^{-7}$ sec.

can be expressed as

$$\tau_{PEM} = \frac{\tau_n + c\tau_p}{1 + c}, \quad (8)$$

$$\tau_{PC} = \frac{\tau_n + \tau_p/b}{1 + 1/b}, \quad (9)$$

where the electron and hole lifetimes τ_n and τ_p are related in terms of the *excess mobile* electron and hole concentrations n and p as follows: $\tau_n/n = \tau_p/p$. True, excess carriers are created in pairs by light, but some of them may be trapped in discrete levels in the forbidden gap: $p = n + n_T$. Here n_T is the concentration of *excess* electrons in trapped states (and is negative in the case that holes are trapped). If carrier trapping is negligible, *viz.*, $|n_T|/n \ll 1$, all of the lifetimes are the same: $\tau_n = \tau_p = \tau_{PEM} = \tau_{PC}$. On the other hand, if the PEM and PC lifetimes are not equal, then it must be that $\tau_n \neq \tau_p$, and consequently a considerable portion of excess carriers must be in trapped states.

The results of lifetime measurements on *p*-type InSb are given in Figs. 3 through 7. Figure 4, in particular, shows that τ_{PEM} and τ_{PC} are identical at higher temperatures but diverge at low temperatures, indicating the trapping of excess carriers in the latter region.

The PEM-PC lifetime difference and also the quenching effects described in the next section are in support of previously published evidence of excess carrier trapping in *p*-type InSb at low temperatures. Wertheim⁸ noted the appearance of "tails" on the exponential curves of photoconductive decay at temperatures below 180°K; Laff and Fan⁹ concluded from the drift and decay of injected pulses of carriers that

⁸ G. K. Wertheim, Phys. Rev. **104**, 662 (1956).

⁹ R. A. Laff and H. Y. Fan, Bull. Am. Phys. Soc. Ser. II, **2**, 347 (1957).

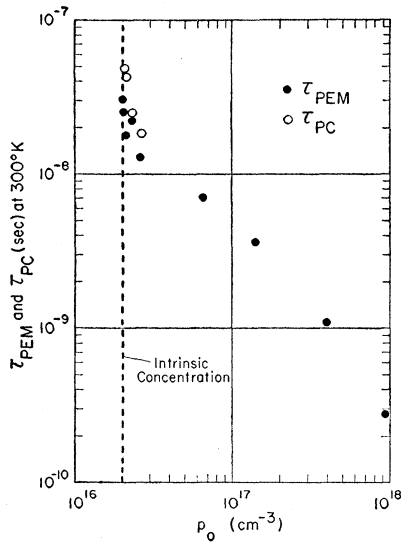


Fig. 7. PEM and PC lifetime vs hole concentration at 300°K.

the majority of excess electrons at 77°K are in trapped states.

(e) Quenching Effects

At low temperatures, if a steady light is directed at a sample in addition to the usual chopped light, strong “quenching” effects are observed. The wave analyzer used to measure photosignals does not respond if only the steady light is on, but when there is chopped light falling on the sample and the steady light is added, a marked decrease in PC response and a marked increase in PEM response is noted. The photoresponses of the purest samples at 77°K would have been quenched by background room-temperature radiation if the Dewar containing the samples had been equipped with infrared-transparent sapphire or rocksalt windows, instead of Pyrex.

A related effect is observed if only chopped light is used and its intensity is varied. In this case it is found that there is strict proportionality of photocurrent to light intensity only if the photon flux density is quite small: less than 10^{14} cm^{-2} sec^{-1} for pure samples, an amount almost invisible to the eye. At higher chopped light intensities the PC response saturates, while the PEM signal varies as some power of intensity greater than unity.

The magnitudes of the quenching effects become smaller with increasing temperature and with increasing impurity concentration, as does the difference between PEM and PC lifetimes; at sufficiently high temperatures, where τ_{PEM} and τ_{PC} are identical, quenching effects are not observed. The strong correlation of quenching with the PEM-PC lifetime difference results because both are due to the trapping of excess carriers. The following section shows how the effects observed can be understood in terms of a particular trap model.

4. RECOMBINATION PROCESSES

The minima and maxima in the PC lifetime curves of Fig. 3 serve to divide the data into three temperature regions: low, middle, and high temperatures. For convenience, each of these regions will be discussed separately.

(a) Low Temperatures

The low-temperature region is characterized by the trapping of excess carriers. From a comparison of electron and hole lifetimes, one can determine whether it is electrons or holes that are being trapped and also the proportion that are in traps under steady-state conditions.

τ_n and τ_p are calculable from the PEM and PC lifetimes. Figure 5 shows that at 77°K, τ_{PEM} is independent of the equilibrium hole concentration, while τ_{PC} varies inversely with p_0 . The samples are extrinsic, so p_0 also represents the net acceptor concentration. When the data are analyzed according to (8), (9), and (2), it is found that the electron and hole lifetimes at 77°K are given by

$$\tau_n = \tau_{\text{PEM}} \cong 2 \times 10^{-10} \text{ sec}, \quad (10)$$

$$\tau_p \cong 25 \tau_{\text{PC}} \cong 1 \times 10^9 / p_0 \text{ sec}, \quad (11)$$

where p_0 is expressed in cm^{-3} . The fraction of excess electrons which are not in trapped states is

$$n / (n + n_T) = \tau_n / \tau_p \cong (2 \times 10^{-19}) p_0.$$

As an example, a sample with 10^{15} cm^{-3} holes has a hole lifetime of one microsecond, five thousand times larger than the electron lifetime, and only 2×10^{-4} of the excess electrons produced by light are mobile.

The results (10) and (11) can be understood in terms of a rather simple model. If the concentration of trapping centers is the same in every sample and if, in the dark, all trap states are unoccupied by electrons at 77°K, then the recombination rate of mobile electrons with empty traps will be the same in all samples, as required by (10). However, τ_p will vary as $1/p_0$, in accord with (11), because the rate at which mobile holes are trapped is proportional to the number of ways a trapped electron can combine with a mobile hole, and there are $p_0 + p \cong p_0$ such holes.

If the trap levels are not too far above the valence band, they will begin to be filled with thermal equilibrium electrons when the temperature is raised from 77°K. There will be fewer empty traps available for the capture of excess electrons and more traps occupied by thermal electrons available for the capture of holes; consequently, it is expected that τ_n will be increased and that τ_p will be decreased. According to (8) and (9), this means that the PEM lifetime will grow larger with rising temperature, while the PC lifetime will decrease first and then increase, since the τ_n term in (9) is negligible at low temperatures but dominates the expression at higher temperature. Moreover, as the

traps fill with thermal electrons, trapping of excess electrons should diminish and the PEM and PC lifetimes should merge.

The data of Figs. 3 and 4 show that lifetimes in the low and middle temperature regions actually behave in the way just described. The quenching effects discussed earlier are understandable too: Background illumination on a sample fills empty traps with electrons (similar to the effect of increased temperature), so the PEM current increases and the PC current decreases.

Quantitatively, the low-temperature lifetime data may be interpreted satisfactorily using the Shockley-Read model¹⁰ of a single level of traps. It will be shown, however, that difficulties are encountered when the same model is used for middle temperatures and that, consequently, more than one trap level may be present in the forbidden band.

Several terms in the Shockley-Read equations can be ignored because the trap concentration N_T must be small compared to the net acceptor concentration in each sample. If N_T were not small compared to $N_A - N_D$, Hall coefficient *vs* temperature data near 77°K would show the effects of trap ionization or de-ionization, and this is not observed. It follows that the Shockley-Read equations for the electron and hole lifetimes may be written as

$$\tau_n = (1+c)^{-1}[\tau_{n0}(1+\alpha) + \tau_{p0}c(1+1/\alpha)], \quad (12)$$

$$\tau_p = \tau_n + \frac{\tau_{p0}N_T}{p_0(1+c)(1+\alpha)}, \quad (13)$$

where c is the ratio n_0/p_0 as usual, and α is defined¹¹ in terms of the energy difference between trap and Fermi level:

$$\alpha = \exp[(E_F - E_T)/kT].$$

The parameters τ_{n0} and τ_{p0} have the definitions given by Shockley and Read.

If the trap level is at least several times kT above the Fermi level in every *p*-type sample at 77°K, the equations for this temperature reduce to

$$\tau_n = \tau_{n0}, \quad (14)$$

$$\tau_p = \tau_n + \tau_{p0}N_T/p_0. \quad (15)$$

(14) and (15) are certainly consistent with the empirical relations (10) and (11), provided the trap concentration is independent of p_0 . Therefore τ_{n0} and τ_{p0} at 77°K are given by

$$\tau_{n0} = 2 \times 10^{-10} \text{ sec}, \quad (16)$$

$$\tau_{p0}N_T = 1 \times 10^9 \text{ sec cm}^{-3}. \quad (17)$$

Earlier it was concluded that the trap concentration must be less than the net acceptor concentration in

every sample. It follows that

$$N_T \lesssim 10^{14} \text{ cm}^{-3},$$

and consequently that at 77°K,

$$\tau_{p0} \gtrsim 10^{-5} \text{ sec}. \quad (18)$$

With the values given in (16) and (17), the Shockley-Read equations (12) and (13), when substituted in (8) (9), predict to within a factor of two all the PEM and PC lifetime data throughout the low-temperature range provided that the trap energy level is set between 0.050 and 0.055 eV from the valence band. However, in the next section the possibility is discussed that there may be more than one trap level in the forbidden band, in which case the value 0.050 eV should be regarded merely as a lower limit to the energy difference between the valence band and the lowest trap level.

(b) Middle Temperatures

In the middle-temperature region, recombination continues to take place through states in the forbidden band. This can be concluded most directly from the fact that within the region, lifetimes are rising strongly with increasing temperature.

If there is only one level of forbidden band states, the Shockley-Read model discussed in the previous section should apply to both middle- and low-temperature data. Over this wide temperature range, an uncertainty is introduced in that one does not know what temperature dependence to ascribe to the trap energy level. However, the uncertainty is avoided if only the data of rather pure samples at the higher temperatures within the middle region are considered; in this case, the Fermi energies are such that values of α somewhat larger than unity can be expected, and the expression for PC lifetime simplifies to one not involving E_T :

$$\tau_{PC} \cong \tau_n \cong \tau_{p0}c/(1+c), \quad (19)$$

where $c = n_0/p_0$. For samples with $p_0 > 10^{16} \text{ cm}^{-3}$, (19) is not quite correct, since the first term in (12) provides a noticeable contribution to τ_{PC} . Incidentally, (19) was used by Wertheim⁸ in the analysis of his data, some of which are presented in Fig. 3 and are seen to agree closely with the present results.

Figure 6 shows that lifetimes at 200°K actually do vary with carrier concentration in the manner described by (19). However, the value of τ_{p0} that must be used to fit the data is

$$\tau_{p0} = 8 \times 10^{-7} \text{ sec} \quad (20)$$

at 200°K.

From a comparison of (20) with the 77°K result (18), it must be concluded that either τ_{p0} (for a single level of traps) decreases by at least an order of magnitude as the temperature rises from 77°K to 200°K, or that over this range there is more than one trap level involved in the recombination of carriers.

Multiple trap levels might be due to the presence of

¹⁰ W. Shockley and W. T. Read, Phys. Rev. **87**, 825 (1952).

¹¹ When the valence or conduction bands are degenerate, a different expression for α must be used.

several different sets of lattice defects (impurity atoms or dislocations) or to a lattice defect for which several charge conditions or "valences" are possible. From the work of Okada,¹² Landsberg,¹³ and Sah and Shockley,¹⁴ it can be shown that only two trap levels, for which the τ_{p0} 's do not vary strongly with temperature, are required to explain the data of both low and middle temperature regions. This result is not too surprising, since the introduction of a second level provides more than enough parameters with which to fit the data.

If only a single level is present, it is necessary to explain the strong temperature dependence of τ_{p0} . The process involved would have to be one in which the probability of hole capture by a trap is at least ten times larger at 200°K than it is at 77°K. The change is too large to be explained by the fact that the average thermal velocity of free holes at 200°K is twice that at 77°K and consequently a hole encounters twice as many traps per unit time at the higher temperature.

It may be that the process by which the energy of capture is dissipated depends strongly on temperature. In this connection, it should be noted that the capture energy itself may change significantly with temperature, since E_T is only about 0.05 eV at 77°K while the band gap itself varies by nearly 0.03 eV between 77°K and 200°K. It is unfortunate that the value of E_T at 200°K is not readily calculated from the available lifetime data.

Effects which can be ruled out as responsible for the temperature dependence of τ_{p0} are screening of the traps due to mobile charge carriers and Auger capture of holes by traps such as described by Bess.¹⁵ In these cases, τ_{p0} might change considerably with temperature through a dependence of the capture probability on carrier concentration, but any such dependence, if assumed, will not be consistent with lifetime vs carrier concentration data (Figs. 5 and 6, for example).

The authors are not aware of any theoretical treatment in the literature predicting the increase with rising temperature of capture probability considered here. The work of Lax,¹⁶ in fact, shows that the capture cross section of some traps will *decrease* with rising temperature, an effect opposite to the one required here.

From lifetime measurements of nickel-doped germanium, Battey and Baum¹⁷ concluded that the capture constants pertaining to the upper acceptor level of nickel have the form $\exp(-A/kT)$, where A is some positive constant. This would satisfy the requirements for τ_{p0} here; however, recent investigations^{12,18} have shown that when the data are properly analyzed in

terms of recombination through both nickel levels, only temperature-independent capture cross sections need be assumed.

It would appear that no clear theoretical justification or experimental precedent can be found for the temperature dependence of τ_{p0} which is necessary if the model of a single level of traps is to be consistent with the lifetime data; consequently there may be some reason to believe that at least two levels of forbidden-band states determine recombination at middle and low temperatures.

(c) High Temperatures

The lifetime curves for different net acceptor concentrations merge into one curve at high temperatures, as shown in Fig. 3. This is understandable because each sample is very nearly intrinsic in its high-temperature range, in which case lifetime is determined by intrinsic carrier concentration, not by net acceptor concentration.

The high-temperature lifetime data are consistent with the hypothesis of a direct interband Auger recombination process, in which the energy of recombination, equal to the energy gap, is taken up by a nearby free electron or hole. Landsberg and Beattie¹⁹ have investigated this effect and find that the lifetime in intrinsic material varies with temperature as

$$\tau \propto \left(\frac{E_G}{kT}\right)^{\frac{3}{2}} \exp\left[\frac{1+2\rho E_G}{1+\rho kT}\right], \quad (21)$$

where ρ is the ratio of electron to hole effective mass m_e/m_h , and E_G is the energy gap. The proportionality factor in (21) is

$$3.8 \times 10^{-18} \epsilon^2 (1+2\rho)(1+\rho)^{\frac{1}{2}} / F^2, \quad (22)$$

where ϵ is the dielectric constant (in cgs units) and F represents two overlap integrals of periodic parts of Bloch functions. Using a Kronig-Penney model, Landsberg and Beattie estimate that F is of the order of one-tenth.

Here it is found that for the value $F=0.04$, (21) and (22) agree well with the experimental results. Figure 3 shows how closely the data are fitted.

Strictly speaking, the above equations apply to a non-degenerate situation, while in fact there is some degeneracy of the conduction band in InSb near 300°K. Nevertheless, the results should not be altered significantly when the degeneracy effect is taken properly into account.

Another process, direct radiative recombination, has often been considered in connection with the lifetime in intrinsic InSb. However, the present data show that the actual variation of lifetime with temperature is quite

¹² J. Okada, J. Phys. Soc. Japan **12**, 1338 (1957).

¹³ P. T. Landsberg, Proc. Phys. Soc. (London) **B70**, 283 (1957).

¹⁴ C. T. Sah and W. Shockley, Phys. Rev. **109**, 1103 (1958).

¹⁵ L. Bess, Phys. Rev. **105**, 1469 (1957).

¹⁶ M. Lax, Bull. Am. Phys. Soc. Ser. II, **1**, 128 (1956); also, *Proceedings of the International Conference on Semiconductors, Rochester, 1958* [J. Phys. Chem. Solids **8**, 166 (1959)].

¹⁷ J. F. Battey and R. M. Baum, Phys. Rev. **100**, 1634 (1955).

¹⁸ S. G. Kalashnikov, *Proceedings of the International Conference on Semiconductors, Rochester, 1958* [J. Phys. Chem. Solids **8**, 52 (1959)].

¹⁹ P. T. Landsberg and A. R. Beattie, *Proceedings of the International Conference on Semiconductors, Rochester, 1958* [J. Phys. Chem. Solids **8**, 73 (1959)].

different from that computed^{8,20} for the radiative lifetime, as can be seen in Fig. 3. In addition, the computed values are too high to be consistent with the data; even at 300°K, the largest lifetimes measured (Fig. 7) are an order of magnitude smaller than the radiative lifetime value. Furthermore, Dumke²¹ has presented arguments to show that because of the high absorption constant for emitted photons in InSb, the direct radiative recombination lifetime is not experimentally observable, except perhaps in extremely thin samples, and that some other lifetime will always be observed, regardless of whether it is smaller or larger than the radiative lifetime.

A possibility that cannot be ruled out entirely is that recombination at high temperatures takes place through forbidden-band states. In this case, an equation of the form (19) would apply, and since each sample is nearly intrinsic in its high-temperature region, (19) becomes

$$\tau = \frac{1}{2} \tau_{p0}.$$

Therefore, the strong temperature dependence of lifetime which is observed at high temperatures would have to be attributed entirely to the variation of τ_{p0} . As pointed out earlier, there is no theoretical support for such a temperature dependence.

Incidentally, it should be noted that the lifetime *vs* hole concentration data at 300°K, as shown in Fig. 7, are representative of all three of the regions (low, middle, and high temperatures) which have been discussed. Therefore, the resulting complexity is too great to allow fruitful analysis of this data.

5. CONCLUSION

The present work has been directed toward an understanding of carrier recombination processes in *p*-type InSb at various temperatures. From analysis of lifetime data, a general picture has emerged: at low temperatures excess electrons are trapped in states in the forbidden band, at middle temperatures trapping becomes negligible but recombination continued to take place through forbidden-band states, while for high temperatures there is the distinct possibility that recombination is predominantly a direct interband Auger effect. Some of the details necessary to complete

this general picture have also been deduced, particularly concerning the states in the forbidden band which determine carrier lifetimes at low temperatures. Thus, it is known that these states are present in the samples studied at an essentially constant concentration not exceeding 10^{14} cm⁻³ and that they have an energy of 0.05–0.06 eV above the valence band at 77°K. Furthermore, since electrons are captured many times more readily than holes, there is probably a strong positive charge on the trap centers at low temperatures.

The present results show also that there may be in fact more than one level of states in the forbidden band through which recombination takes place. It is quite possible that a single type of "multivalent" lattice defect is present, with a charge of perhaps +2 or +3 at 77°K but becoming less positive as the temperature (and Fermi level) rises; in other words, these defects introduce into the forbidden band a series of states with progressively smaller electron capture constants and progressively larger hole capture constants. Alternatively, there may be several sets of lattice defects present which introduce entirely independent levels.

Perhaps the foremost question remaining to be answered concerns the identity of the lattice defects in InSb. The fact that the concentration of the low-temperature traps is the same in all the samples studied suggests that the traps may be associated with a fundamental structural property of the InSb lattice—for example, some type of lattice disorder phenomenon. On the other hand, the introduction of traps may be simply a characteristic property of the method of preparation of InSb crystals by pulling from the melt. In any event, it is significant that the trap concentrations are the same in crystals grown over a period of several years with varying extraction and rotation rates, some doped with cadmium or zinc and others not intentionally doped; furthermore, the InSb used was zone refined in various ways and was prepared from indium and antimony purified by various procedures.

A final point to be noted in this connection is the close agreement of the present results with those reported by Wertheim⁸—a fact which is significant because the InSb used by Wertheim was not prepared at this laboratory. The agreement of the two sets of data implies that the same forbidden-band states are present in both sets of samples to approximately the same concentration.

²⁰ I. M. Mackintosh and J. W. Allen, Proc. Phys. Soc. (London) **B68**, 985 (1955); D. W. Goodwin and T. P. McLean, Proc. Phys. Soc. (London) **B69**, 689 (1956).

²¹ W. P. Dumke, Phys. Rev. **105**, 139 (1957).